



Contents lists available at ScienceDirect

Arabian Journal of Chemistry

journal homepage: www.ksu.edu.sa

Plausible effect of hesperetin and nano-hesperetin against bisphenol-A induced hepatotoxicity in a rat model

Khawlah Sultan Alotaibi^a, Mai Elobeid^a, Promy Virk^{a,*}, Manal Ahmed Awad^b, Malak Abdullah Al-Qahtani^a, Doaa Mohamed Elnagar^a

^a Department of Zoology, College of Sciences, King Saud University, P.O. Box 22452, Riyadh 11459, Saudi Arabia

^b King Abdullah Institute for Nanotechnology, King Saud University, Riyadh 11451, Saudi Arabia

ARTICLE INFO

Keywords:

Bisphenol A
Hesperetin
Oxidative stress
Inflammation
Nanoparticles
Green synthesis

ABSTRACT

Bisphenol A (BPA) is a non-persistent, anthropic compound and continues to be ubiquitous in the environment. Since BPA is estrogenic in nature, its exposure induces adverse cellular responses associated with oxidative stress and inflammation. Hesperetin, a major flavonoid present in lemons and sweet oranges exhibits a broad spectrum of pharmacological effects attributed to its potent anti-inflammatory and antioxidant status. The current study reports the 'green' synthesis of nano hesperetin (NHsp) followed by characterization that included; Fourier Transform Infrared spectroscopy (FTIR), X-Ray Diffraction (XRD), Transmission Electron Microscopy (TEM), Scanning Electron Microscopy (SEM) and Dynamic Light Scattering (DLS). In accordance with the findings, the mean size of the synthesized nanoparticles was 139.9 nm with a PDI of 0.362. The morphotype was primarily spherical and rod shaped. This was followed by a comparative assessment of the ameliorative efficacy of bulk and nano hesperetin against BPA-induced hepatotoxicity in rat. The findings showed that post-exposure to 250 mg/kg of BPA for 21 days significantly enhanced the pro-inflammatory cytokines (IL-6, IL-8, IL-1 β , TNF- α), in the serum with a concomitant upregulation in the mRNA expression of Nrf 2 (Nuclear factor erythroid 2-related factor) factor in the liver. Treatment with both bulk hesperetin (Hst) and nano hesperetin (NHst) reduced the levels of cytokines and expression of hepatic Nrf2 factor. This was paralleled by the modulatory effects on the histology of liver and kidney which were reversed on treatment. Taken together, the nano hesperetin was more efficacious in alleviating the BPA-induced toxicity. Thus, hesperetin and its nano formulation could be potentially promising nutraceuticals in medicine and industry.

1. Introduction

Natural or synthetic compounds that adversely impact the endocrine system by causing a disarray in the endogenous hormone production and functions have been termed as xenoestrogens or endocrine disruptors (Schug et al., 2016, Ma et al., 2019). Bisphenol A (BPA) is one such xenoestrogen, being globally used in the manufacture various polymers; epoxy resins, plastics etc. From 2016 through 2022, a gross annual growth rate of about 4.8 % has been recorded. The wide range of its use in polycarbonate plastics and epoxy resins which are being used in every industry was also cited as a reason for the output expansion to 10.7 million metric tons by 2020. In 2022, it is predicted that there will be a USD 22.49 billion global demand for BPA (Manzoor et al., 2022). The substance is prevalent in all environmental compartments (air, land, and water), which expands the channels via which people might be

exposed to it (Meli et al., 2020). Asia Pacific accounts for about 52 % of the global BPA market, with the United States and Europe producing the remaining 36 % (Almeida et al., 2018). Due to this, it has a plethora of applications in consumer products used in everyday life (Vasiljevic and Harner, 2021, Xing et al., 2022). Additionally, BPA is a common constituent in several consumer products such as food and drinking bottles or cans containers that leads to its leaching out at under high temperatures and acidic or basic conditions adding to its human exposure (Elswefy et al., 2016). Since BPA has a hormone-like feature, it may lead to impaired cellular responses associated with oxidative stress and inflammations that trigger the immune system, which are key elements in its pathogenesis (Jang et al., 2020). The rising incidence of several types of cancers has been associated with BPA exposure (Manzoor et al., 2022). The enhanced estrogenic activity reveals the carcinogenic molecular action of BPA, according to several prior *in vivo* investigations

* Corresponding author.

E-mail address: bvirk@ksu.edu.sa (P. Virk).

<https://doi.org/10.1016/j.arabjc.2023.105563>

Received 30 June 2023; Accepted 12 December 2023

Available online 14 December 2023

1878-5352/© 2023 The Authors. Published by Elsevier B.V. on behalf of King Saud University. This is an open access article under the CC BY-NC-ND license (<http://creativecommons.org/licenses/by-nc-nd/4.0/>).

(such as mice, rats, etc.) (Rubin, 2011). According to a recent study, BPA exposure decreased the amount of the protein Nrf2/Keap1 in male mice more than in female mice, making male mice more vulnerable to the hepatic oxidative stress caused by BPA (Müller et al., 2018).

Additionally, the plasma and colon tissues of BPA-exposed mice had increased amounts of reactive oxygen species (ROS and proinflammatory cytokines (Wang et al., 2021a, 2021b).

As the production and consumption of products containing BPA continues to grow with a concomitant environmental exposure, natural compounds such as flavonoids with a potent antioxidant status can alleviate the BPA toxicity. Several studies have been reviewed and it has been reported that the flavonoids could be potential BPA-detoxifying agents attributed to their wide spectrum of pharmacological benefits such as antioxidant activity, anti-inflammatory, hepatoprotective, anti-apoptotic-modulatory, and their ability to activate the immune system (Amjad et al., 2020). The biological activity of flavonoids is due to functional hydroxyl groups and the ability to catalyze electron transport and scavenge free radicals (Yao et al., 2004, Rahal et al., 2014, Khan et al., 2018). Hesperetin (3',5,7-Trihydroxy-4'-methoxyflavanone) is one of such flavonoid and is a potent antioxidant in citrus fruits. It belongs to the flavanone class of flavonoids and is extracted mainly from peel of citrus fruits. Several studies have reported the efficacy of hesperetin against certain pathological conditions, exhibiting its anti-inflammatory and antioxidant properties (Khan et al., 2020). However, despite its proven pharmacological actions in humans, its poor physicochemical and biopharmaceutical properties have restricted its status to be recognized, which is mainly due to its limited oral bioavailability from conventional dosage forms (Pollard et al., 2006, Ratnam et al., 2006, Yang et al., 2012). However, nanotechnology has been a promising approach in the therapeutic use of phytochemicals as it enhances the bioavailability of natural antioxidants which is the current trend and forefront of research in nanomedicine. There has been a plethora of studies on the use of natural plant based bioactive compounds in the fabrication of nanoparticles either in conjugation with metals or in pure form (Yadav et al., 2020; Liu et al., 2023). The core concept of green synthesis is the redox reaction, in which an organism's constituent parts or its extract convert metal ions to stable nanoparticles. In addition, the process of reducing particles to the nanoscale, known as "nanonization," increases the surface area, which raises its saturation solubility and rate of dissolution, subsequently leading to enhanced bioavailability. Several modes of nanonization of phytochemicals have been reported along with their efficacious therapeutic applications (Ghosh et al., 2022; Kapoor-Narula and Lenka, 2022).

Moreover, biogenic synthesis of nanoparticles; based on using microorganisms and phytochemicals; also, being non-metallic provide an environmentally benign, reliable, and sustainable mode of synthesis. In order to enhance the antioxidant activity and provide a targeted distribution of the bio constituents that otherwise exhibit poor cell permeability and internalization, nanoparticles functionalized with natural antioxidants act as the carriers for these phytochemicals (Khalil et al., 2019). There have been several studies on nano formulations of hesperidin and hesperetin, the major bioflavonoids in citrus fruits (Kheradmand et al., 2018, Elmoghayer et al., 2023; Stanisic et al., 2020; Simão et al., 2020). After being nanonized, hesperidin nanoparticles were used to create stable nano emulsions to be used for topical application as a face cream (Stanisic et al., 2020). Furthermore, hesperetin-loaded nano lipid carriers demonstrated remarkable *in vitro* cytotoxic effect of on glioblastoma cells (Simão et al., 2020). Hence, the present study evaluates the antioxidative efficacy of hesperetin, and it is nano-formulation against bisphenol-A-induced hepatotoxicity in a male rat model. The process of nanonization intended on keeping the essence of green credentials and includes no metallic component and chemical surfactants/ stabilizers. The mode of 'green synthesis' employed was granted a patent in 2016 (Elobeid et al., 2016).

Table 1

Experimental design.

Experimental group	
Group I (Control)	negative control
Group II (BPA)	administered BPA only (250 mg/Kg/day) (Huang et al., 2019)
Group III (nano-Hst)	administered nano-hesperetin only (50 mg/Kg/day) (Elobeid et al., 2016).
Group IV (BPA + Hst)	administered BPA and treated with nano-hesperetin (50 mg/kg/day).
Group V (BPA + nano-Hst)	administered BPA and treated with nano-hesperetin (50 mg/kg/day).

2. Materials and methods

2.1. Chemicals

Bisphenol A (>99 % purity) was procured from Tokyo Chemical Industry (TCI) and hesperetin (>98 % purity) from Shaanxi Huike Botanical Development Co. (Xi'an, China). Commercial (ELISA) Kits for interleukins; (IL) -6, IL-8, and IL-1 β , tumor necrosis factor (TNF- α) were purchased from MyBioSource Inc. (USA), and the Nrf2 primers from Macrogen Inc. (Seoul, Korea).

2.2. Synthesis of nano-hesperetin

Nano hesperetin was synthesized by the nanoprecipitation technique as reported by Elobeid et al. (2016). Hesperetin powder (100 mg) was dissolved in 25 mL of methanol to form a solution, which was then added to boiling water under ultrasonic conditions to form a mixture. About 1–2 mL of the hesperetin-methanol solution was sprayed into about 70 mL boiling water dropwise with a flow rate of 0.3 mL/min within 5 min under ultrasonic conditions. After sonication for about 10–20 min, the solution was then stirred at about 800 rpm at room temperature for about 20–30 min to obtain hesperetin nanoparticles. The mass of Hst nanoparticles was collected and dried for a day under the hood to obtain a required concentration for the *in vivo* study.

2.3. Characterization of hesperetin nano particles

The synthesis of nano-Hst particles was characterized through Zita-sizer to measure the average size of the synthesized nano hesperetin particles. The nanoparticle's shape, morphologies, and nano surfaces were imaged by Transmission Electron Microscopy (TEM) and Scanning Electron Microscope (SEM). X-Ray Diffraction (XRD) determined the crystallographic structure. Also, the functional groups of Hst particles and bulk were recognized by Fourier Transform Infrared (FTIR) Spectroscopy.

2.4. Animals

The animal house facility at King Saud University, Riyadh, Saudi Arabia provided adult albino rats (n = 25) weighing 300 \pm 150 g for the exposure study which was conducted complying to the animal ethics committee. The rats were divided into five experimental groups (5 rats in each group) for a three-week exposure period after acclimating to the laboratory environment for a week (temperature: 22 $^{\circ}$ C, 12-hour photoperiod). Rats had unlimited access to tap water and were given commercial chow. The experimental groups were administered an oral dose of BPA and treated with hesperetin (Hst) and nano hesperetin (Nano-Hst) daily through the experimental period. Bisphenol A and hesperetin were dissolved in 2 % ethanol and administered daily by oral gavage (Table 1).

After three weeks, blood samples were collected from all animals. After the animals were sacrificed; the liver and kidney were excised out. For histological investigation liver and kidney samples were fixed in 10

Table 2The primer sequences for *Nrf2* and *gapdh* genes.

Gene Name	Forward Primer	Reverse Primer
<i>Nrf2</i>	5'-CAC ATC CAG ACA GAC ACC AGT -3'	5'-CTA CAA ATG GGA ATG TCT CTG C -3'
<i>gapdh</i>	5'-AGG TTG TCT CCT GTG ACT TC -3'	5'-CTG TTG CTG TAG CCA TAT TC -3'

% formalin, and then embedded in paraffin blocks. Sections with a thickness of approximately 3–4 μm were routinely stained with hematoxylin and eosin (H&E). In addition, liver samples and sera were stored at $-80\text{ }^{\circ}\text{C}$ for the bioassays.

2.5. Estimation inflammatory and oxidative stress biomarkers

Tumor necrosis factor (TNF-) and interleukin (IL) -6, IL-8, and IL-1 levels were assessed in the serum using commercial ELISA kits in line with the manufacturer's recommendations. Furthermore, using GAPDH as a housekeeping gene, RT-PCR was utilized to assess the hepatic mRNA expression of nuclear factor erythroid 2 (NFE-2) -related factor 2 (Nrf2) as a biomarker of oxidative stress (Table 2). The conventional 2- $\Delta\Delta\text{Ct}$ technique was used to determine the relative amount of mRNA.

2.6. Histopathological analysis

2.6.1. Hepatic histopathological scoring system

Liver sections stained by H&E were subjected to scoring system in accordance with the Pathology Committee of NASH Clinical Research Network (Aldahmash et al., 2016).

Ballooning, none = 0, few balloon cells = 1, many cells = 2, prominent balloon cells = 3. Inflammation, none = 0, <2 foci per 400 field = 1, 2–4 foci per 400 field = 2, >4 foci per 400 field = 3.

Steatosis, normal (<5%) = 0, 5–33 % = 1, 33–66 % = 2 and > 66 % = 3. The results revealed as 0 = normal, 1 = mild, 2 = moderate and 3 = severe.

2.6.2. Renal histopathological scoring system

Histopathological scoring system was achieved on kidney sections stained by H&E (Toprak et al., 2020).

Glomerular zone: No damage = 0, thickening of Bowman capsule = 1, retraction of glomerular tuft = 2, glomerular fibrosis = 3.

Tubular zone: No damage = 0, tubular brush border loss (less than 25 %) = 1, tubular brush border loss (more than 25 %) = 2, inflammation and casts = 3.

2.7. Statistical analysis

Data is illustrated as mean and standard error (SE). The Tukey's test was performed to analyze group differences using a one-way ANOVA. The significant value was $p \leq 0.05$ (SPSS 22.0, Chicago, Illinois, USA).

3. Results

3.1. Characterization of hesperetin nanoparticles

3.1.1. Size and morphology

As shown in Fig. 1 the average size of the Hst nanoparticle was $139.9 \pm 43.40\text{ nm}$ with a poly-dispersity index (PDI) of 0.362, observed as a single peak.

Both TEM and SEM microscopy were used to determine the morphology of nano-Hst as shown in Fig. 2. The micrographs display agglomerated particles that are predominantly spherical and rod-shaped and have distinct varied morphotype. The spherical nanoparticles had an average diameter of 69 nm (Fig. 2A, B, C and D).

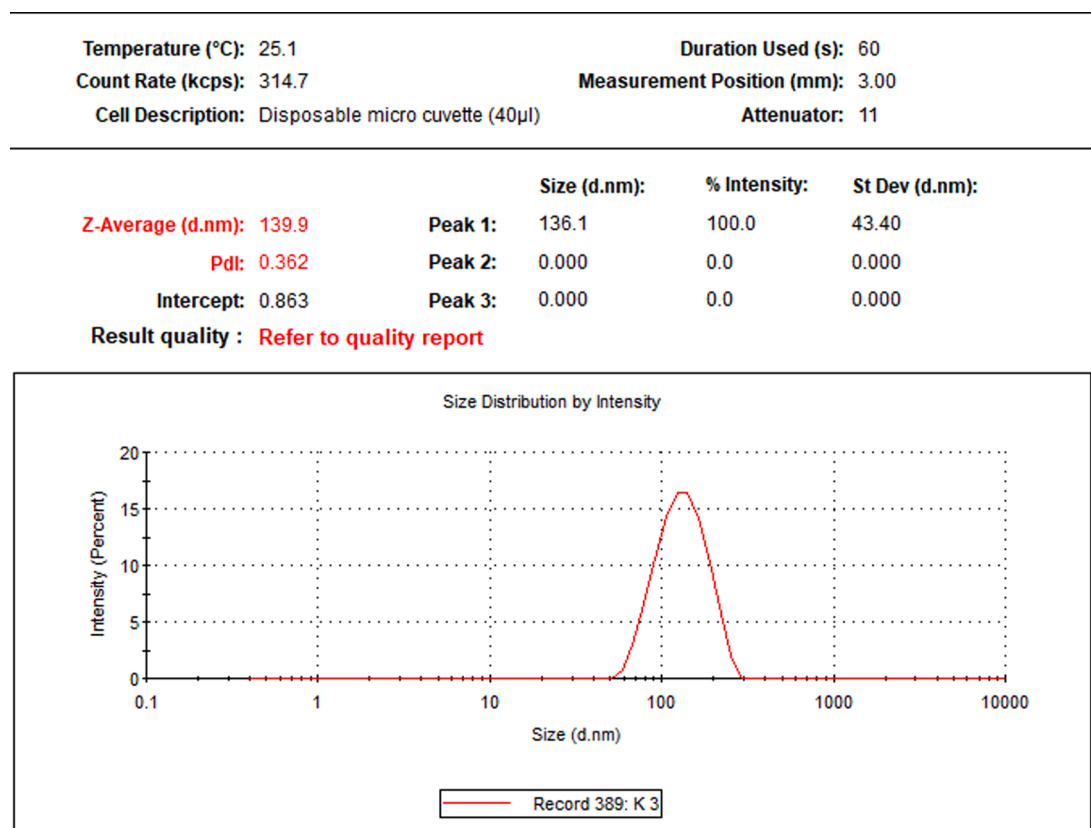


Fig. 1. Particle size distribution of the nano-hesperetin.

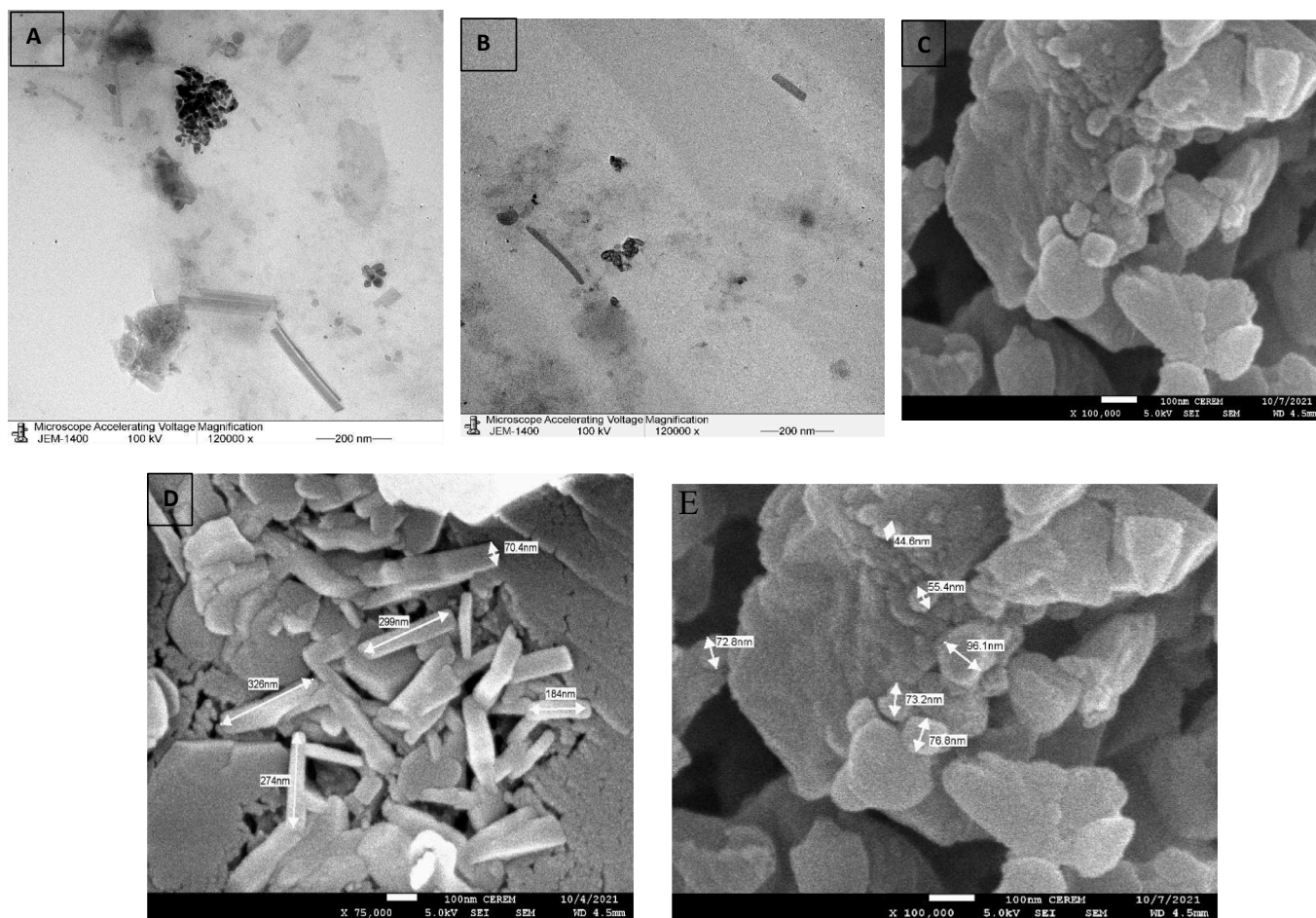


Fig. 2. A and B show the micrographs (TEM), C,D and E show the scanning electron microscope (SEM) of the nanoparticles of hesperetin.

Bulk & Nano-Hst

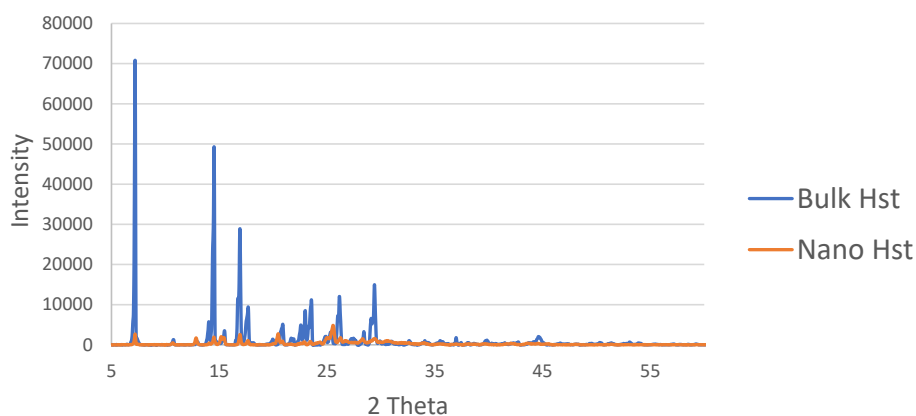


Fig. 3. X-ray diffractograms of the bulk and nano-hesperetin.

3.1.2. X-ray diffractometer (XRD)

The X-ray diffractograms of the bulk Hst and nano Hst illustrated that the intensity of the peaks was less in nano-Hst, which indicates an amorphous structure of nanoparticles. Furthermore, since the peaks observed for both the bulk and the nano-Hst were at the same position which is attributed to the similar chemical composition of the two samples (Fig. 3).

3.1.3. Fourier Transform Infrared spectroscopy (FTIR)

According to Fig. 4, the FTIR spectra identified the potential biomolecules of bulk and nano-Hst. The bulk and nano-Hst spectra were remarkably similar, indicating that the nano scaling process did not alter the chemical structure of the compound. Noticeable IR bands were observed for the bulk-Hst at 3497.47 cm^{-1} , 1639.11 cm^{-1} , 1583.13 cm^{-1} , 1305.11 cm^{-1} , 1175.25 cm^{-1} , 818.51 cm^{-1} , and 742.30 cm^{-1} . Identical bands were illustrated for the nano-Hst. In the bulk-Hst

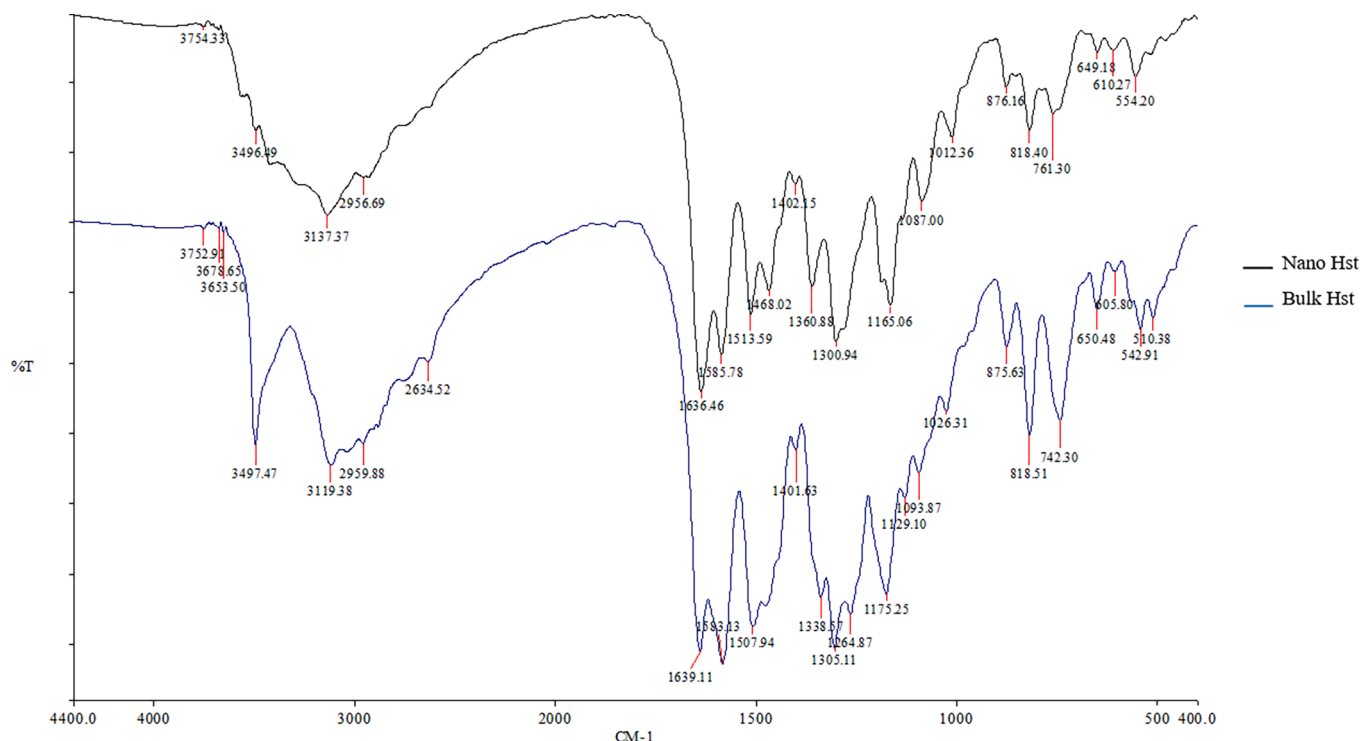


Fig. 4. FTIR spectra of the bulk and nano-hesperetin.

spectra, the strong and broad band in the 3550–3200 cm^{-1} area corresponded to hydrogen-bonded O–H stretching identified alcohol compound. The band at 1648–1638 cm^{-1} indicate alkene compound with strong C=C stretching. Further, peaks between 1600 cm^{-1} and 1585 cm^{-1} were indicate C–C stretch were identified as aromatics. The band at 1310–1250 cm^{-1} with strong C–O stretching was attributed to aromatic ester compound. The band at 1205–1124 cm^{-1} identified a strong C–O stretching with tertiary alcohol compound. Finally, the bands at 840–790 cm^{-1} was ascribed to alkene with medium C=C bending.

3.2. Bioassays

3.2.1. Concentration of pro-inflammatory cytokines (IL-6, IL-8, IL-1 β and TNF- α)

In comparison to the control group (42.1 ± 0.6 pg/ml), exposure to BPA significantly ($p \leq 0.05$) increased serum levels of IL-6 (56.5 ± 0.3 pg/ml). Both the bulk Hst treatment (45.8 ± 0.7 pg/ml) and the nano-Hst treatment (41.3 ± 2.9 pg/ml) considerably ($p \leq 0.05$) decreased the concentrations. Between the control group and the group that received the nano-Hst, there was no discernible change (Fig. 5A). In addition, the serum levels of IL-8 considerably ($p \leq 0.05$) increased (52.6 ± 2.5 pg/ml) on exposure to BPA. The serum concentrations of IL-8 were considerably ($p \leq 0.05$) decreased with co-administration of both bulk Hst (39.3 ± 0.3 pg/ml) and nano- Hst (37.8 ± 0.4 pg/ml)(Fig. 5B). Additionally, IL-1 β was significantly ($p \leq 0.05$) elevated on BPA exposure (6.9 ± 0.2 pg/ml). Co-administration of both bulk Hst (4.84 ± 0.192 pg/ml) and nano hesperetin (3.4167 ± 0.0998 pg/ml) showed a significant ($p \leq 0.05$) reduction in the concentrations. Nevertheless, nano-Hst was more effective (Fig. 5C). Significantly higher TNF- α levels (111.7 ± 0.7 pg/ml) were observed as compared to the control (99.9 ± 0.7 pg/ml).Co-administration of both bulk Hst (105.5 ± 2.1 pg/ml) and nano- Hst (102.7 ± 1.0 pg/ml) significantly ($p \leq 0.05$) declined the TNF- α concentrations (Fig. 5D).Among the treatments, however, there was no discernible difference observed.

3.2.2. mRNA expression of nuclear factor- erythroid 2 (NFE2) -related factor 2 (Nrf2) in liver

A significant fold change in the expression of hepatic mRNA of Nrf-2 in was observed on BPA exposure in comparison to the control. Treatment with nano- Hst (0.6 ± 0.1) and only nano- Hst (0.7 ± 0.1) significantly ($p \leq 0.05$) downregulated the mRNA expression of Nrf2 compared to BPA exposed group (1.7 ± 0.3) (Fig. 6).

3.3. Histopathological investigation

3.3.1. Liver

Untreated control liver sections showed normal appearance with an anastomose network of hepatocytes with abundant central nuclei, also tissue revealed binucleated cells referring to regeneration (Fig. 7A). Additionally, liver of rats treated with nano-Hst displayed the same feature of untreated control liver (Fig. 7B). Whereas, liver sections from the group exposed to BPA exhibited severe steatosis both micro and macro-vesicular with dilatation of sinusoids (Fig. 7C). Meanwhile, sections of rats from the BPA + Hst group showed marked improvement with almost healthy and less steatosis (Fig. 7D). Moreover, rats treated with BPA + nano Hst revealed less steatosis compared to control and a few numbers of inflammatory cells (Fig. 7E). Hepatic pathological score showed increasing levels of liver pathology to severe changes in the BPA group due to increasing ballooning, inflammation and steatosis. Whereas, treated groups; BPA + Hst and BPA + nano Hst revealed less pathological score as changes decreased (Table 3).

3.3.2. Kidneys

Untreated control kidney showed normal renal structure with abundant spherical glomeruli in between proximal and convoluted tubules in the cortex area (Fig. 8A). Additionally, the renal tissue of rats treated with nano- Hst showed the same structure as the untreated control (Fig. 8B). While sections exposed BPA revealed intense degeneration of glomeruli and tubules with increased glomerular space due to the severe degeneration. Additionally, the tubules looked faint and very thin (Fig. 8C). Meanwhile, rats from the BPA + Hst group revealed

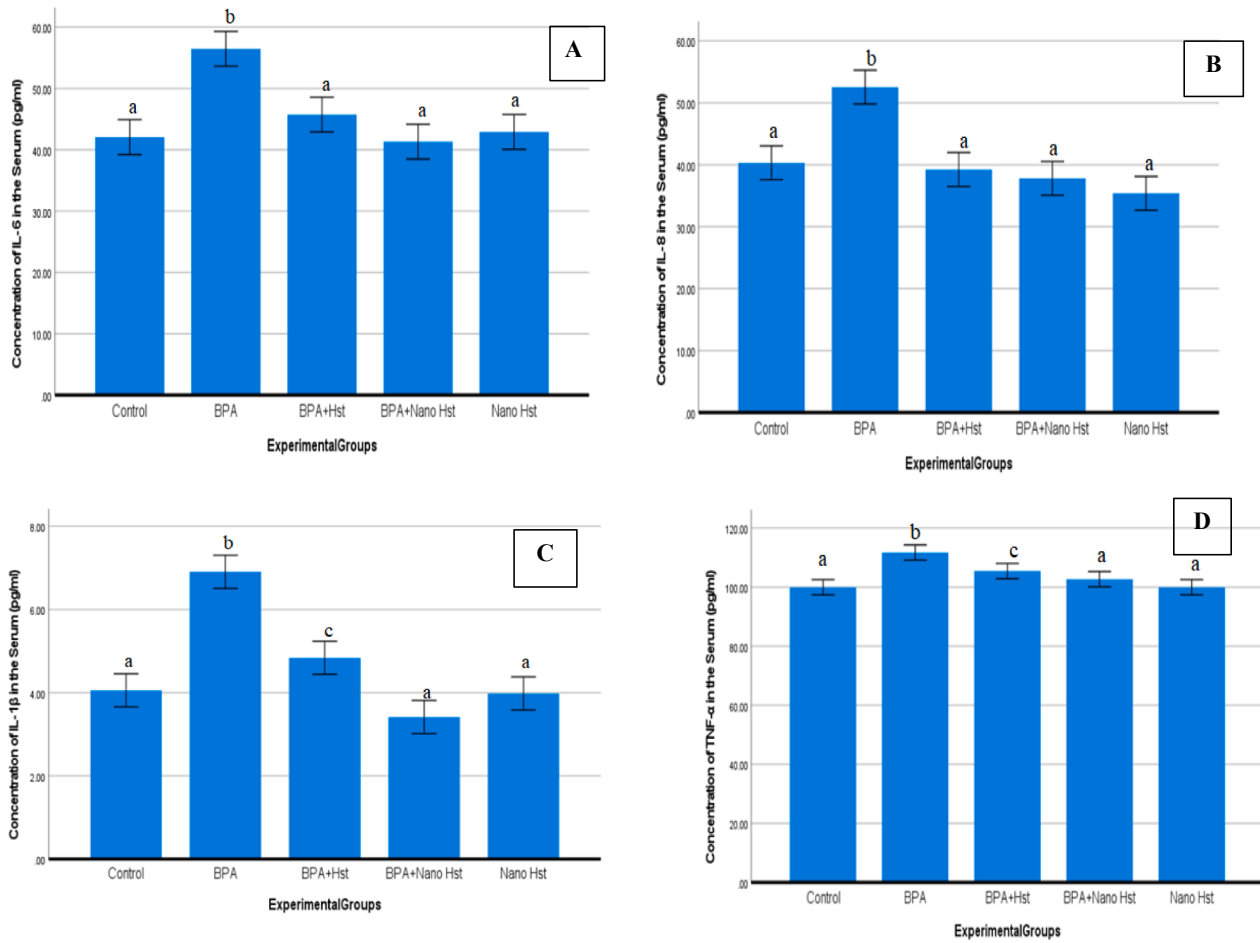


Fig. 5. Mean (\pm SE) the concentration levels of (A) IL-6 (pg/ml), (B) IL-8 (pg/ml), (C) IL-1 β (pg/ml), (D) TNF- α (pg/ml) in serum of rats exposed to BPA and treated with hesperetin (Hst) and nano hesperetin (NHst). Different letters indicate a significant ($p \leq 0.05$) difference between the experimental groups.

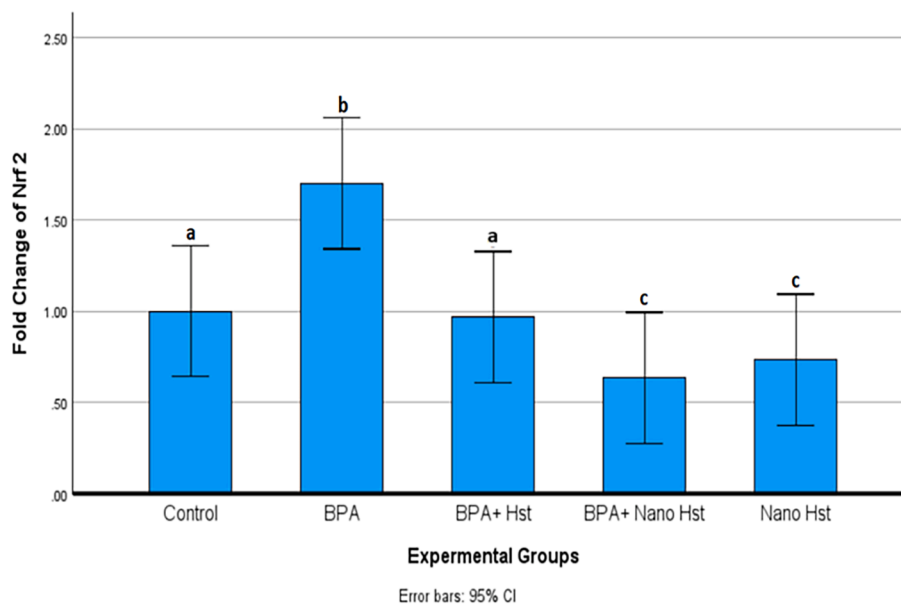


Fig. 6. Mean (\pm SE) mRNA expression of nuclear factor-erythroid 2 (NFE2)-related factor 2 (Nrf2) of rats exposed to BPA and treated with hesperetin (Hst) and nano hesperetin (NHst). Different letters signify a difference that is statistically significant ($p < 0.05$) between the experimental groups.

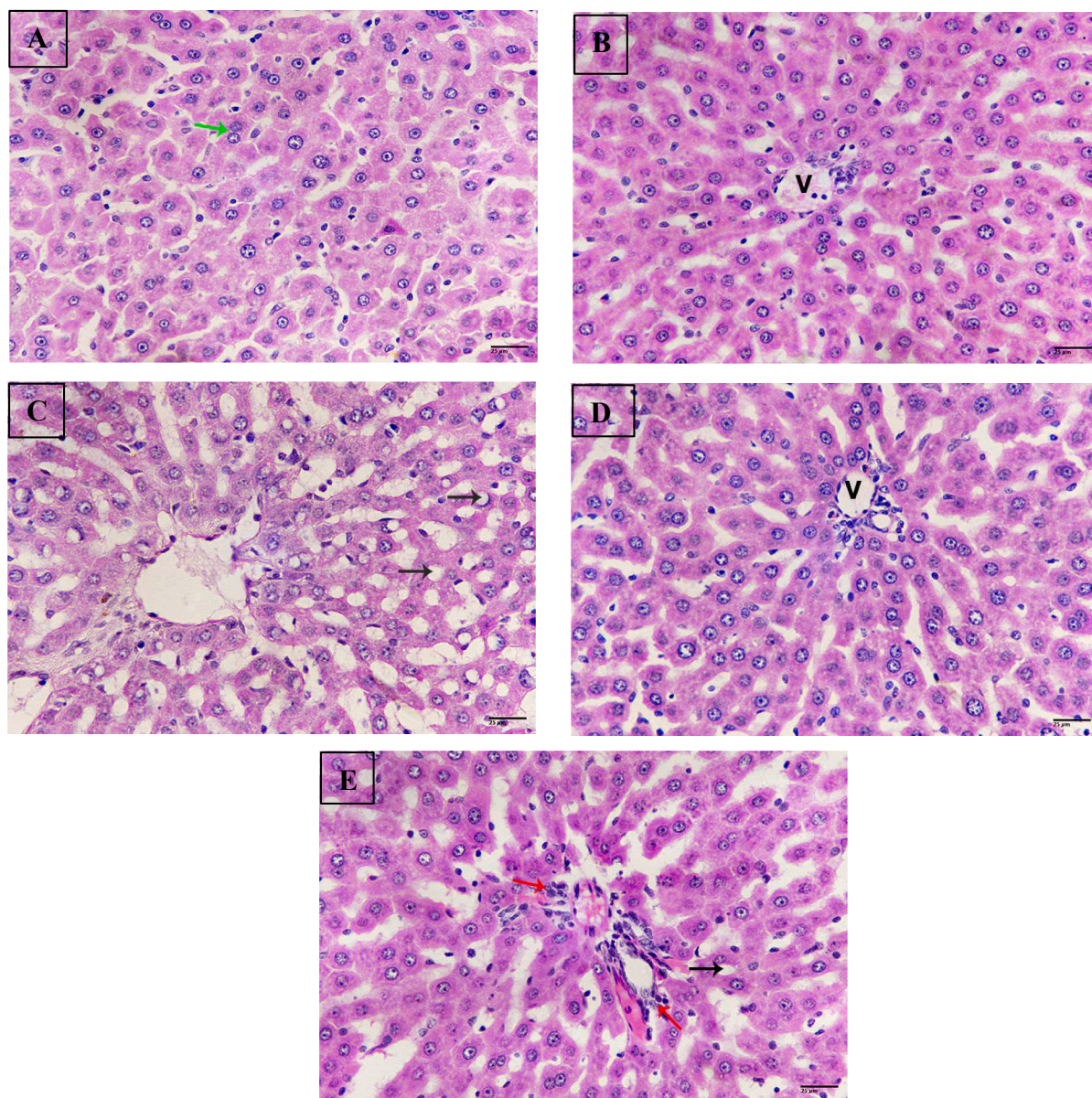


Fig. 7. Photomicrograph of liver sections. (A) Sections from untreated control liver showing normal structure, binucleated cells (green arrow). (B) Sections of rat liver treated with nano hesperetin revealing normal structure, central vein (V). (C) Sections from rat liver treated with bisphenol A exhibiting severe steatosis (black arrows). (D) Sections from rat liver treated with BPA + hesperetin displaying normal tissue, vein (V). (E) Sections of rat liver treated with bisphenol A + nano-hesperetin showing improvement, less steatosis (black arrow), inflammatory cells (red arrows). (H&E-400X)(scale bar 25 μm .).

Table 3
Hepatic pathological score.

Groups	Ballooning	Inflammation	Steatosis
Control	0	0	0
Nano-Hst	0	0	0
BPA	2	2	3
BPA + Hst	1	1	2
BPA + nano-Hst	1	1	1

almost normal renal tissue with healthy glomeruli and tubules (Fig. 8D). Moreover, renal tissue of rats treated with BPA + nano-Hst showed only slight improvement compared to control group (Fig. 8E). The group exposed to BPA displayed increasing of renal pathological score of glomerular and tubular zones as retraction of the glomerular tuft and loss of tubular brush borders besides increasing of inflammation and tubular casts. Meanwhile, the treated groups; BPA + Hst and BPA +

nano-Hst exhibited less renal pathological score due to improvement of the renal tissue (Table 4).

4. Discussion

A 'green synthesis' of hesperetin nanoparticles was successfully reported keeping the 'clean technology' as the pivotal point since the technique did not make use of any chemical surfactants and stabilizers. The chemical groups mapped in hesperetin were similar in both the bulk and nano Hst as the mode of synthesis included only nano scaling of the flavonoid. The obtained average size of hesperetin nanoparticles is from 139.9 nm, with mainly spherical and rod-shaped particles, respectively, which is in line with the previous study reported by Elobeid et al. (Elobeid et al., 2016). The XRD analysis showed the crystalline structure of bulk and nano-Hst, with the nano-Hst having low intensity contrary to bulk Hst, which revealed an amorphous state of nano-Hst, which facilitates diffusion and solubility (Lazer et al., 2018). Although there were

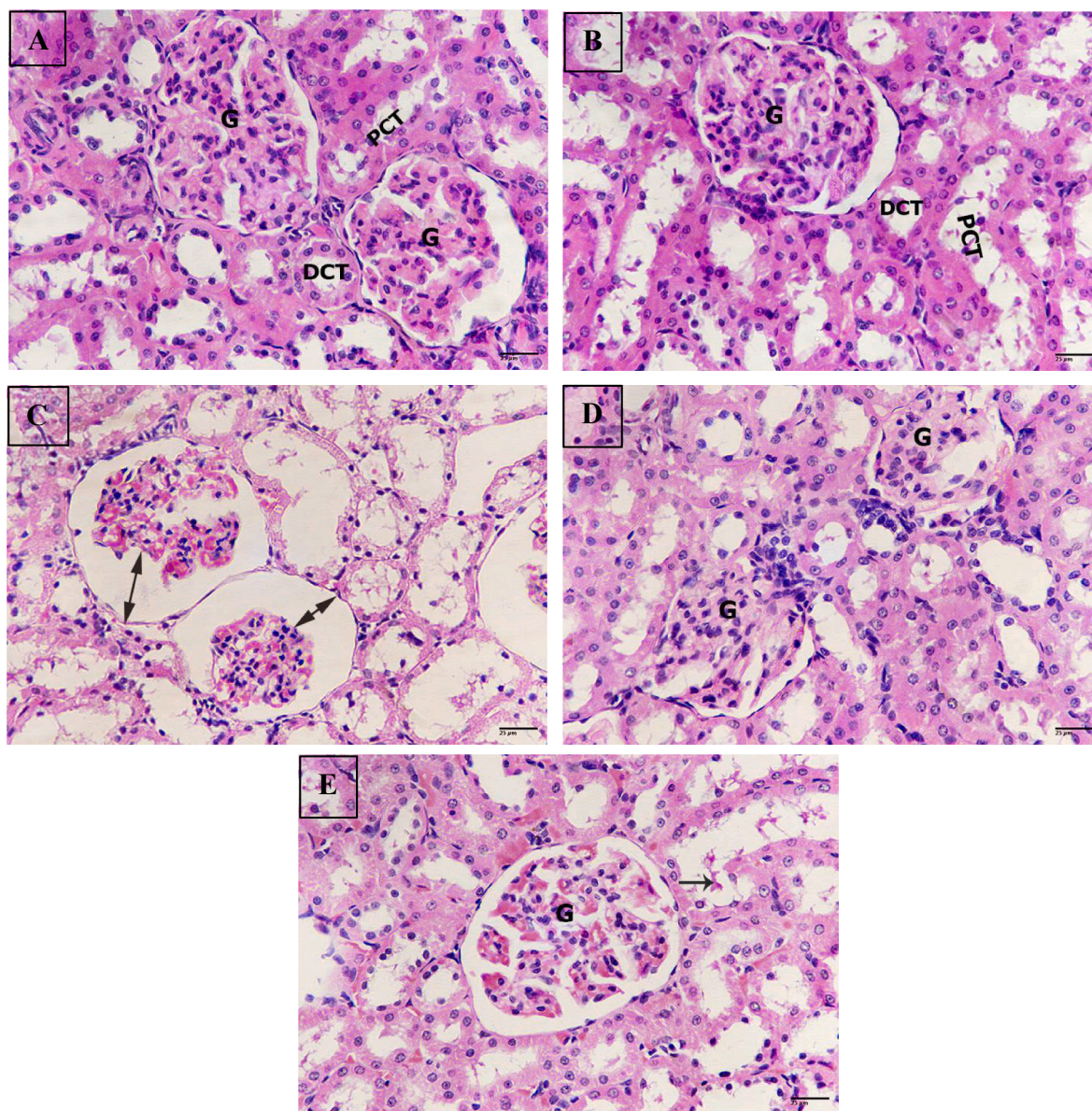


Fig. 8. Photomicrograph of kidney sections. (A) Sections from untreated control renal tissue displaying normal structure, glomerulus (G), proximal convoluted tubules (PCT), distal convoluted tubules (DCT). (B) Sections of rat kidney treated with nano hesperetin showing healthy structure, glomerulus (G), proximal convoluted tubules (PCT), distal convoluted tubules (DCT). (C) Sections of rat kidney treated with bisphenol A revealing severe degeneration, increasing of the glomerular space (double headed arrows). (D) Sections of rat kidney treated with bisphenol A + hesperetin displaying marked improvement, glomerulus (G). (E) Sections from rat kidney treated with bisphenol A + nano hesperetin posting some improvement, glomerulus (G), tubular cast (black arrow). (H&E-400X)(scale bar 25 μm).

Table 4
Renal pathological score.

Groups	Glomerular zone	Tubular zone
Control	0	0
Nano-Hst	0	0
BPA	1–2	2–3
BPA + Hst	2	1
BPA + nano- Hst	2	2–3

slight variations in the pattern and intensity of the nano-Hst spectra, the FTIR spectra revealed similar functional groups in both bulk and nano-Hst (Paramita et al., 2022). Previous literature has reported that induction of pro-inflammatory cytokines including IL-6, IL-1 β , TNF- α , and IFN- β by the endocrine disrupting chemicals (EDCs) which are defined as

substances, either natural or man-made, that have the ability to mimic, inhibit, or interfere with the endocrine system (Popescu et al., 2021). A study in the recent times by Pan et al. (Pan et al., 2023) reported that BPA exposure in porcine intestinal epithelial cells perturbed the oxidant/antioxidant status leading to oxidative stress/damage with a parallel proinflammatory response. In consensus with this, the findings of the present study show that exposure to BPA (250 mg/Kg) elicited the enhanced production of IL-6, IL-8, IL-1 β , and TNF- α . Studies have reported that cell apoptosis is the major signal pathway involved in the BPA-induced tissue damage, including the brain (Caglayan et al., 2022), liver (Gu et al., 2021), and lung (Liu et al., 2016). Furthermore, Wang et al demonstrated a dose-dependent increase in the TNF- α and IL-6 levels on BPA exposure (Wang et al., 2021a, 2021b). On the contrary, according to Lu et al. (Lu et al., 2019), exposure to a low dose of BPA triggers the expression of pro-inflammatory cytokines such as TNF- α and IL-6.

Nuclear factor (erythroid-derived 2)-like 2 (Nrf2) and nuclear factor- κ B (NF- κ B) are two important transcription factors that control cellular reactions to oxidative stress and inflammation, respectively. According to research, Nrf2 and NF- κ B are important pathways that regulate the equilibrium of cellular redox status and inflammatory stress responses. This molecular cross-talk between the components explains why these pathways are so important (Wardyn et al., 2015). In the current investigation, BPA exposure caused the hepatic Nrf2 mRNA expression to increase, reflecting oxidative damage. A number of toxic insults / diseases that are normally linked to oxidative stress have shown a contributing role of Nrf2, which has emerged as a key regulator of oxidative resistance (Ma, 2013).

Treatment with nano Hst and bulk Hst effectively attenuated and suppressed the Nrf2 expression. Nevertheless, the treatments showed no observable difference. A previous study showed that rats treated with hesperetin had no effect on Nrf2 expression, while a decrease in the expression of Nrf2 protein was reported (Miler et al., 2020). The anti-inflammatory effect of hesperetin is re-attributed to reduced ROS overproduction through the Nrf2 pathway (Kubatka et al., 2021). This explains the role of hesperetin in alleviating inflammation which was demonstrated in the present study. Treatment with both bulk Hst and nano Hst significantly lowered the serum levels of pro-inflammatory cytokines. Taken together, the effect of the nano Hst was more pronounced than the bulk Hst. The protective and inhibitory effect of hesperetin is well recognized on inflammation. These findings are in line with other studies on the role of hesperetin in attenuating oxidative damage and inflammatory responses. (Li et al., 2021a, Li et al., 2021b).

The histopathological investigation in the current study demonstrated that the sections of liver exposed to BPA showed severe steatosis and dilatation of sinusoids, which indicates the abnormal retention of lipids within hepatocytes, attributed to the accumulative nature of bisphenol A (Al-Mustafa and Al-Sultan, 2022). Furthermore, exposed to BPA caused hemorrhage in the central vein, degenerated and vacuolized hepatocytes with pyknotic nuclei, and lymphocyte aggregation (Eweda et al., 2019). Besides, treatment with both bulk Hst and nano Hst reversed these effects and alleviated the steatosis, inflammation, degeneration and necrosis of hepatocytes, and function of the liver (Wan et al., 2020, Li et al., 2021a, 2021b). Furthermore, the H&E staining result showed intense degeneration of glomeruli and tubules, with increasing glomerular space due to the severe degeneration in the sections of kidneys from the group exposed to BPA (Korriem, 2022). Additionally, treatment the rats treated with Hst revealed a well maintained renal tissue with healthy glomeruli and tubules. This is in congruence with previous study that showed the similar histopathological alterations in rats induced by BPA (Shi et al., 2021). The ameliorative effect of Hst was also observed cisplatin-induced acute kidney injury (Chen et al., 2019). In addition, the pathological score for both hepatic and renal tissue mirrored the histopathological alterations. The effects of the nanosized Hst were not very conspicuous over the bulk, which could be due to the short period of exposure and treatment. However, the nano-Hst proved to be comparable in efficacy with the bulk and could potentially be a nanosized form with enhanced available to its intended biological destination. There have been several reports in the past few years which have recognized the pharmacological role of the flavonoid, Hst in attenuating oxidative stress, restoring cellular antioxidant status, inflammatory response and apoptosis (Baradaran et al., 2020). In addition, several forms of nanoparticles of the flavonoid with lipid carriers or metals compounds have been formulated using varied methods of synthesis and their enhanced efficacy has been highlighted both in *in vivo* and *in vitro* studies (Baradaran et al., 2020; Khalaj et al., 2018; Kheradmand et al., 2018). The above mentioned studies have primarily reported the neuroprotective effect of nano crystals of Hst against oxido-inflammatory stress in the brain. In congruence with these reports, the key findings of the present study elucidated the counteractive effect of both Hst and nano Hst against BPA toxicity. The nano formulation reported demonstrates an amalgamation of green chemistry

and nanoscience using an environmentally acceptable solvent; methanol. Thus, these findings offer a novel therapeutic approach to combat oxidative damage/inflammatory response induced by the continual exposure to plasticizers in our daily life in the current times.

5. Conclusion

The cornerstone of green synthesis is the capacity of organic substances such as phytocompounds to stabilize them into nanoparticles. The nano-formulation in the present study does offer a novel green synthesis of nanoparticles with substantial advantages over the traditional methods of nanosization; the prime advantage is being environmentally benign, economical and facile. The pro-inflammatory cytokines (IL-6, IL-8, IL-1b, TNF) were enhanced with a parallel increase in Nrf2 mRNA expression, clearly illustrating an inflammatory response elicited by the induction of oxidative stress by BPA. Treatment with hesperetin and its nano- formulation was efficacious in attenuating these modulations. Considering that hesperetin, a bioflavonoid has been widely recognized for its broad spectrum of pharmacological benefits, its nanonization sans chemicals could be advantageous in therapeutic strategies. Furthermore, the mode of nano formulation followed a sustainable approach making the process facile, safe and environmentally acceptable.

Declaration of competing interest

The authors declare that they have no known competing financial interests or personal relationships that could have appeared to influence the work reported in this paper.

Acknowledgements

The authors extend their appreciation to the Deputyship for Research and Innovation, "Ministry of Education" in Saudi Arabia for funding this research (IFKSUOR3-242-3).

References

- Aldahmash, B.A., El-Nagar, D.M., Ibrahim, K.E., 2016. Attenuation of hepatotoxicity and oxidative stress in diabetes STZ-induced type 1 by biotin in Swiss albino mice. *Saudi J. Biol. Sci.* 23 (2), 311–317. <https://doi.org/10.1016/j.sjbs.2015.09.027>.
- Almeida, S., Raposo, A., Almeida-González, M., et al., 2018. Bisphenol A: food exposure and impact on human health. *Compr. Rev. Food Sci. Food Saf.* 17, 1503–1517. <https://doi.org/10.1111/1541-4337.12388>.
- Al-Mustafa, S.S., Al-Sultan, R.G., 2022. Histological changes of liver and lung induced by bisphenol A in pregnant mice. <https://doi.org/10.25258/ijddt.12.2.37>.
- Amjad, S., Rahman, M.S., Pang, M.G., 2020. Role of antioxidants in alleviating bisphenol A toxicity. *Biomolecules* 10, 1105. <https://doi.org/10.3390/biom10081105>.
- Baradaran, S., Ghasemi-Kasman, M., Moghaddam, A.H., 2020. Nano-hesperetin enhances the functional recovery and endogenous remyelination of the optic pathway in focal demyelination model. *Brain Res. Bull.* 164, 392–399. <https://doi.org/10.1016/j.brainresbull.2020.09.006>.
- Caglayan, C., Kandemir, F.M., Ayna, A., et al., 2022. Neuroprotective effects of 18 β -glycyrrhethinic acid against bisphenol A-induced neurotoxicity in rats: involvement of neuronal apoptosis, endoplasmic reticulum stress and JAK1/STAT1 signaling pathway. *Metab. Brain Dis.* 37, 1931–1940. <https://doi.org/10.1007/s11011-022-01027-z>.
- Chen, X., Wei, W., Li, Y., et al., 2019. Hesperetin relieves cisplatin-induced acute kidney injury by mitigating oxidative stress, inflammation and apoptosis. *Chem. Biol. Interact.* 308, 269–278. <https://doi.org/10.1016/j.cbi.2019.05.040>.
- Elmoghayer, M.E., Saleh, N.M., Abu Hashim, I.I., 2023. Enhanced oral delivery of hesperidin-loaded sulfobutylether- β -cyclodextrin/chitosan nanoparticles for augmenting its hypoglycemic activity: in vitro-in vivo assessment study. *Drug Deliv. and Transl. Res.* <https://doi.org/10.1007/s13346-023-01440-6>.
- Elobeid, L. A., Manal Awad, et al., 2016. Synthesis of hesperetin nanoparticles. Patent 9700512B1. Available from: <https://patents.google.com/patent/US9700512B1/en>.
- Elswefy, S.E., Abdallah, F.R., Atteia, H.H., et al., 2016. Inflammation, oxidative stress and apoptosis cascade implications in bisphenol A-induced liver fibrosis in male rats. *Int. J. Exp. Pathol.* 97, 369–379. <https://doi.org/10.1111/iep.12207>.
- Eweda, S., Newairy, A., Abdou, H., et al., 2019. Bisphenol A-induced oxidative damage in the hepatic and cardiac tissues of rats: the modulatory role of sesame lignans. *Exp. Ther. Med.* <https://doi.org/10.3892/etm.2019.8193>.

- Ghosh, S., Nandi, S., Basu, T., 2022. Nano-antibacterials using medicinal plant components: an overview. *Front. Microbiol.* 22 (12), 768739 <https://doi.org/10.3389/fmicb.2021.768739>.
- Gu, Z., Jia, R., He, Q., et al., 2021. Alteration of lipid metabolism, autophagy, apoptosis and immune response in the liver of common carp (*Cyprinus carpio*) after long-term exposure to bisphenol A. *Ecotoxicol. Environ. Saf.* 211, 111923 <https://doi.org/10.1016/j.ecoenv.2021.111923>.
- Huang, Y., Wu, C., Ye, Y., et al., 2019. The increase of ROS caused by the interference of DEHP with JNK/p38/p53 pathway as the reason for hepatotoxicity. *Int. J. Environ. Res. Public Health* 16. <https://doi.org/10.3390/ijerph16030356>.
- Jang, J.-W., Lee, J.-W., Yoon, Y.D., et al., 2020. Bisphenol A and its substitutes regulate human B cell survival via Nrf2 expression. *Environ. Pollut.* 259, 113907 <https://doi.org/10.1016/j.envpol.2019.113907>.
- Kapoor-Narula, U., Lenka, N., 2022. Chapter 9 - Phytochemicals and their nanoformulation in sustained drug delivery and therapy. In: Thatoi, H., Mohapatra, S., Das, S.K., (Eds.) *Innovations in Fermentation and Phytopharmaceutical Technologies*, Elsevier, pp. 181-220. <https://doi.org/10.1016/B978-0-12-821877-8.00019-1>.
- Khalaj, R., Moghaddam, A.H., Zare, M., 2018. Hesperetin and its nanocrystals ameliorate social behavior deficits and oxido-inflammatory stress in rat model of autism. *Int. J. Dev. Neurosci.* 69, 80–87. <https://doi.org/10.1016/j.ijdevneu.2018.06.009>.
- Khalil, L., Yehye, W.A., Etxeberria, A.E., et al., 2019. Nanoantioxidants: recent trends in antioxidant delivery applications. *Antioxidants (Basel)* 9. <https://doi.org/10.3390/antiox9010024>.
- Khan, A., Ali, T., Rehman, S.U., et al., 2018. Neuroprotective effect of quercetin against the detrimental effects of LPS in the adult mouse brain. *Front. Pharmacol.* 9 <https://doi.org/10.3389/fphar.2018.01383>.
- Khan, A., Ikram, M., Hahm, J.R., et al., 2020. Antioxidant and anti-inflammatory effects of citrus flavonoid hesperetin: special focus on neurological disorders. *Antioxidants (Basel)* 9. <https://doi.org/10.3390/antiox9070609>.
- Kheradmand, E., Moghaddam, A.H., Zare, M., 2018. Neuroprotective effect of hesperetin and nano-hesperetin on recognition memory impairment and the elevated oxygen stress in rat model of Alzheimer's disease. *Biomed. Pharmacother.* 97, 1096–1101. <https://doi.org/10.1016/j.biopha.2017.11.047>.
- Koriem, K.M.M., 2022. Fetic acid amends bisphenol A-induced toxicity, DNA breakdown, and histopathological changes in the liver, kidney, and testis. *World J. Hepatol.* 14, 535. <https://doi.org/10.4254/wjh.v14.i3.535>.
- Kubatka, P., Mazurakova, A., Samec, M., et al., 2021. Flavonoids against non-physiological inflammation attributed to cancer initiation, development, and progression—3PM pathways. *EPMA J.* 12, 559–587. <https://doi.org/10.1007/s13167-021-00257-y>.
- Lazer, L.M., Sadhasivam, B., Palaniyandi, K., et al., 2018. Chitosan-based nanoformulation enhances the anticancer efficacy of hesperetin. *Int. J. Biol. Macromol.* 107, 1988–1998. <https://doi.org/10.1016/j.ijbiomac.2017.10.064>.
- Li, S., Shao, L., Fang, J., et al., 2021b. Hesperetin attenuates silica-induced lung injury by reducing oxidative damage and inflammatory response. *Exp. Ther. Med.* 21 <https://doi.org/10.3892/etm.2021.9728>.
- Li, J., Wang, T., Liu, P., et al., 2021a. Hesperetin ameliorates hepatic oxidative stress and inflammation via the PI3K/AKT-Nrf2-ARE pathway in oleic acid-induced HepG2 cells and a rat model of high-fat diet-induced NAFLD. *Food Funct.* 12, 3898–3918. <https://doi.org/10.1039/d0fo02736g>.
- Liu, S.-H., Su, C.-C., Lee, K.-I., et al., 2016. Effects of bisphenol A metabolite 4-Methyl-2, 4-bis (4-hydroxyphenyl) pent-1-ene on lung function and type 2 pulmonary alveolar epithelial cell growth. *Sci. Rep.* 6, 1–11. <https://doi.org/10.1038/srep39254>.
- Liu, L., Yu, C., Ahmad, S., Ri, C., 2023. Preferential role of distinct phytochemicals in biosynthesis and antibacterial activity of silver nanoparticles. *Journal of Environmental Management* 344, 118546.
- Lu, X., Li, M., Wu, C., et al., 2019. Bisphenol A promotes macrophage proinflammatory subtype polarization via upregulation of IRF5 expression in vitro. *Toxicol. In Vitro* 60, 97–106. <https://doi.org/10.1016/j.tiv.2019.05.013>.
- Ma, Q., 2013. Role of nrf2 in oxidative stress and toxicity. *Annu. Rev. Pharmacol. Toxicol.* 53, 401–426. <https://doi.org/10.1146/annurev-pharmtox-011112-140320>.
- Ma, Y., Liu, H., Wu, J., et al., 2019. The adverse health effects of bisphenol A and related toxicology mechanisms. *Environ. Res.* 176, 108575 <https://doi.org/10.1016/j.envres.2019.108575>.
- Manzoor, M.F., Tariq, T., Fatima, B., et al., 2022. An insight into bisphenol A, food exposure and its adverse effects on health: a review. *Front. Nutr.* 9, 1047827. <https://doi.org/10.3389/fnut.2022.1047827>.
- Meli, R., Monnolo, A., Annunziata, C., et al., 2020. Oxidative stress and BPA toxicity: an antioxidant approach for male and female reproductive dysfunction. *Antioxidants* 9, 405. <https://doi.org/10.3390/antiox9050405>.
- Miler, M., Živanović, J., Ajdžanović, V., et al., 2020. Citrus flavanones upregulate thymroph Sirt1 and differentially affect thyroid Nrf2 expressions in old-aged Wistar rats. *J. Agric. Food Chem.* 68, 8242–8254. <https://doi.org/10.1021/acs.jafc.0c03079>.
- Müller, S.G., Jardim, N.S., Quines, C.B., et al., 2018. Diphenyl diselenide regulates Nrf2/Keap-1 signaling pathway and counteracts hepatic oxidative stress induced by bisphenol A in male mice. *Environ. Res.* 164, 280–287. <https://doi.org/10.1016/j.envres.2018.03.006>.
- Pan, Z., Huang, J., Hu, T., et al., 2023. Protective effects of selenium nanoparticles against bisphenol A-induced toxicity in porcine intestinal epithelial cells. *Int. J. Mol. Sci.* 24, 7242. <https://doi.org/10.3390/ijms24087242>.
- Paramita, P., Sethu, S.N., Subhadrappa, N., et al., 2022. Neuro-protective effects of nano-formulated hesperetin in a traumatic brain injury model of Danio rerio. *Drug Chem. Toxicol.* 45, 507–514. <https://doi.org/10.1080/01480545.2020.1722690>.
- Pollard, S.E., Whiteman, M., Spencer, J.P., 2006. Modulation of peroxynitrite-induced fibroblast injury by hesperetin: a role for intracellular scavenging and modulation of ERK signalling. *Biochem. Biophys. Res. Commun.* 347, 916–923. <https://doi.org/10.1016/j.bbrc.2006.06.153>.
- Popescu, M., Feldman, T.B., Chitnis, T., 2021. Interplay between endocrine disruptors and immunity: implications for diseases of autoreactive etiology. *Front. Pharmacol.* 12, 165. <https://doi.org/10.3389/fphar.2021.626107>.
- Rahal, A., Kumar, A., Singh, V., et al., 2014. Oxidative stress, prooxidants, and antioxidants: the interplay. *Biomed Res. Int.* 2014, 761264 <https://doi.org/10.1155/2014/761264>.
- Ratnam, D.V., Ankola, D.D., Bhardwaj, V., et al., 2006. Role of antioxidants in prophylaxis and therapy: a pharmaceutical perspective. *J. Control. Release* 113, 189–207. <https://doi.org/10.1016/j.jconrel.2006.04.015>.
- Rubin, B.S., 2011. Bisphenol A: an endocrine disruptor with widespread exposure and multiple effects. *J. Steroid Biochem. Mol. Biol.* 127, 27–34. <https://doi.org/10.1016/j.jsbmb.2011.05.002>.
- Schug, T.T., Johnson, A.F., Birnbaum, L.S., et al., 2016. Minireview: endocrine disruptors: past lessons and future directions. *Mol. Endocrinol.* 30, 833–847. <https://doi.org/10.1210/me.2016-1096>.
- Shi, R., Liu, Z., Liu, T., 2021. The antagonistic effect of bisphenol A and nonylphenol on liver and kidney injury in rats. *Immunopharmacol. Immunotoxicol.* 43, 527–535. <https://doi.org/10.1080/08923973.2021.1950179>.
- Simão, D., Honorato, T., Gobo, G., Piva, H., Goto, P., et al., 2020. Preparation and cytotoxicity of lipid nanocarriers containing a hydrophobic flavanone. *Colloids Surf. A: Physicochem. Eng. Aspects* 601. <https://doi.org/10.1016/j.colsurfa.2020.124982ff>.
- Stanisic, D., Liu, L.H.B., Dos Santos, R.V., Costa, A.F., Durán, N., Tasic, L., 2020. New sustainable process for hesperidin isolation and anti-ageing effects of hesperidin nanocrystals. *Molecules* 25 (19), 4534. <https://doi.org/10.3390/molecules25194534>.
- Toprak, T., Sekerci, C.A., Aydin, H.R., Ramazanoglu, M.A., Arslan, F.D., Basok, B.I., Kucuk, H., Kocakogol, H., Aksoy, H.Z., Ascı, S.S., et al., 2020. Protective effect of chlorogenic acid on renal ischemia/reperfusion injury in rats. *Arch. Ital. Urol. Androl.* 92, 153.
- Vasiljevic, T., Harner, T., 2021. Bisphenol A and its analogues in outdoor and indoor air: properties, sources and global levels. *Sci. Total Environ.* 789, 148013 <https://doi.org/10.1016/j.scitotenv.2021.148013>.
- Wan, J., Kuang, G., Zhang, L., et al., 2020. Hesperetin attenuated acetaminophen-induced hepatotoxicity by inhibiting hepatocyte necrosis and apoptosis, oxidative stress and inflammatory response via upregulation of heme oxygenase-1 expression. *Int. Immunopharmacol.* 83, 106435 <https://doi.org/10.1016/j.intimp.2020.106435>.
- Wang, K., Qiu, L., Zhu, J., et al., 2021a. Environmental contaminant BPA causes intestinal damage by disrupting cellular repair and injury homeostasis in vivo and in vitro. *Biomed. Pharmacother.* 137, 111270 <https://doi.org/10.1016/j.biopha.2021.111270>.
- Wang, S., Yang, Y., Luo, D., et al., 2021b. Bisphenol A increases TLR4-mediated inflammatory response by up-regulation of autophagy-related protein in lung of adolescent mice. *Chemosphere* 268, 128837. <https://doi.org/10.1016/j.chemosphere.2020.128837>.
- Wardyn, J.D., Ponsford, A.H., Sanderson, C.M., 2015. Dissecting molecular cross-talk between Nrf2 and NF-κB response pathways. *Biochem. Soc. Trans.* 43, 621–626. <https://doi.org/10.1042/BST20150014>.
- Xing, J., Zhang, S., Zhang, M., et al., 2022. A critical review of presence, removal and potential impacts of endocrine disruptors bisphenol A. *Comp. Biochem. Physiol. C: Toxicol. Pharmacol.* 109275 <https://doi.org/10.1016/j.cbpc.2022.109275>.
- Yadav, N., Parveen, S., Banerjee, M., 2020. Potential of nano-phytochemicals in cervical cancer therapy. *Clinica Chimica Acta* 5, 60–72. <https://doi.org/10.1016/j.cca.2020.01.035>.
- Yang, H.L., Chen, S.C., Senthil Kumar, K.J., et al., 2012. Antioxidant and anti-inflammatory potential of hesperetin metabolites obtained from hesperetin-administered rat serum: an ex vivo approach. *J. Agric. Food Chem.* 60, 522–532. <https://doi.org/10.1021/jf2040675>.
- Yao, L.H., Jiang, Y.-M., Shi, J., et al., 2004. Flavonoids in food and their health benefits. *Plant Foods Hum. Nutr.* 59, 113–122. <https://doi.org/10.1007/s1130-004-0049-7>.